

is even more striking as may be noted from the broken line of *Figure 1* and from the triangular data points. The fatigue lifetime values,  $N_f$ , shown here were obtained under alternating tension-compression at a stress amplitude  $\sigma_a$ , of 17.2 MPa. For the two lower molecular weight samples, the log  $N_f$  values are based on the test data reported by Sauer *et al.*<sup>3</sup> while, for the highest molecular weight polymer, the plotted values are estimated lifetimes based on extrapolation of test data obtained at a higher stress amplitude (20.7 MPa) and at a lower stress amplitude (13.8 MPa).

It is evident from *Figure 1* that the average fatigue lifetime rises by over 3 decades as the molecular weight rises from  $10^5$  to  $2 \times 10^6$ ; this occurs despite the fact that this range of molecular weights is well above the estimated entanglement molecular weight of polystyrene, viz. 35 000 (ref 15). This marked improvement in fatigue performance with increase of molecular weight is attributed primarily to a greater resistance to craze breakdown. Although crazes are less extensive and slower to develop at the lower levels of stress involved in fatigue fracture as compared to static fracture, they nevertheless play an important role in the

fracture process<sup>8,16</sup>. Studies of the fatigue fracture surface of polystyrene by scanning electron microscopy show that the fatigue crack invariably initiates in a surface craze which itself developed in response to a high local stress concentration, and then advances and propagates through the process of craze breakdown<sup>3,8</sup>. With increase in chain length and with reduction in the number of chain ends there is a greater degree of chain entanglement and of orientation hardening in the plastically deformed craze microfibrils. If, however, as discussed more fully in a separate publication<sup>17</sup>, the increase in molecular weight is produced through crosslinking, and with little change in  $\bar{M}_n$  or chain end density, then no improvement in either ultimate strength or in fatigue lifetime is achieved.

#### Acknowledgements

This research was supported by National Science Foundation Grant No. DMR-74-02444.

J. A. Sauer

Department of Engineering Science,  
Oxford University,  
Oxford, UK

(On sabbatical leave from Rutgers  
University, New Brunswick, NJ, USA)  
(Received 2 March 1978)

#### References

- 1 Vlachopoulos, J., Hadjis, N. and Hamielec, A. E. *Polymer* 1977, 19, 115
- 2 Foden, E., Morrow, D. R. and Sauer, J. A. *J. Appl. Polym. Sci.* 1972, 16, 519
- 3 Sauer, J. A., Foden, E. and Morrow, D. R. *Polym. Eng. Sci.* 1977, 17, 246
- 4 Flory, P. J. *J. Am. Chem. Soc.* 1945, 67, 2048
- 5 Bueche, F. 'Physical Properties of Polymers', Interscience, New York, 1962
- 6 Vincent, P. I. *Polymer* 1960, 1, 425
- 7 Zhurkov, S. N. *Int. J. Fract.* 1975, 11, 629
- 8 Sauer, J. A., McMaster, A. D. and Morrow, D. R. *J. Macromol. Sci. (B)* 1976, 12, 561
- 9 Hoare, J. and Hull, D. *Phil. Mag.* 1972, 26, 443
- 10 Lainchbury, D. L. G. and Bevis, M. *J. Mater. Sci.* 1976, 11, 2222
- 11 Murray, J. and Hull, D. *J. Polym. Sci. (A-2)* 1970, 8, 1521
- 12 Fox Jr, T. G. and Flory, P. J. *J. Appl. Phys.* 1950, 21, 581
- 13 Rudin, A. and Burgin, D. *Polymer* 1975, 16, 291
- 14 McCormick, H. W., Brewer, F. M. and Kin, L. *J. Polym. Sci.* 1959, 39, 87
- 15 Gent, A. N. and Thomas, A. G. *J. Polym. Sci. (A-2)* 1972, 10, 571
- 16 Kambour, R. P. *Macromol. Rev.* 1973, 7, 1
- 17 Warty, S., Sauer, J. A., and Charlesby, A. to be published

## Melt viscosity and thermal properties of poly(ethylene oxide) fractions and blends

### Introduction

The temperature dependence of the isothermal growth rate of spherulites and the overall crystallization kinetics of fractions of poly(ethylene oxide) with different molecular weights has recently been studied by one of the authors<sup>1</sup>. In a forthcoming paper we will report a study on the crystallization kinetics of blends of fractions of poly(ethylene oxide)<sup>2</sup>.

In this Letter the temperature dependence of the kinematic viscosity of fractions of poly(ethylene oxide) over a range of molecular weight from 1000 to 20 000, and of their relative blends has been studied in order to determine some correlation between molecular and thermodynamic parameters of the melt state and kinetic and thermodynamic quantities normally used in describing the crystallization behaviour of polymers. The present work is preliminary to a more

complete and detailed study on crystallization kinetics and thermal and mechanical properties of blends of PEO, which is in progress.

### Experimental

Zero shear viscosity ( $\eta_0$ ) and density ( $\rho$ ) were measured on monodisperse melted fractions of poly(ethylene oxide) (PEO) in the range of molecular weight from  $10^3$  (PEO 1) to  $20 \times 10^3$  (PEO 20). The PEO samples were produced by Fluka AG. Viscosity was measured by a cone and plate Shirley-Ferranti viscometer at temperatures ranging from 40°–110°C. A quartz plummet suspended from the hook of an analytical balance was immersed in the melted samples to determine the relative densities. In this way it was possible to calculate the density over the same range of temperature. Viscosity and density measurements were also performed on blends of  $2 \times 10^3$

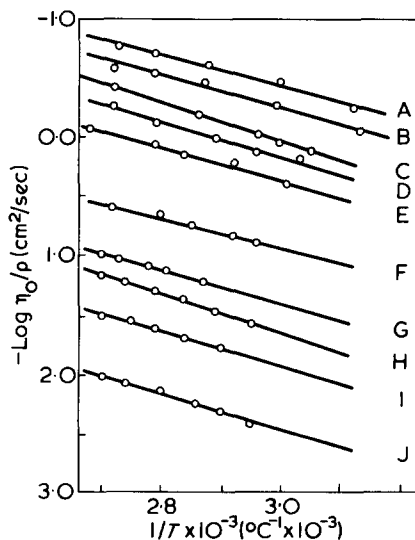


Figure 1 Cologarithm of kinematic viscosity,  $\eta_0/\rho$ , at vanishing shear rate versus  $1/T$  for different molecular weight fractions of PEO, as indicated: A, 1000; B, 1550; C, 2000; D, 3000; E, 4000; F, 6000; G, 9000; H, 10 000; I, 15 000; J, 20 000

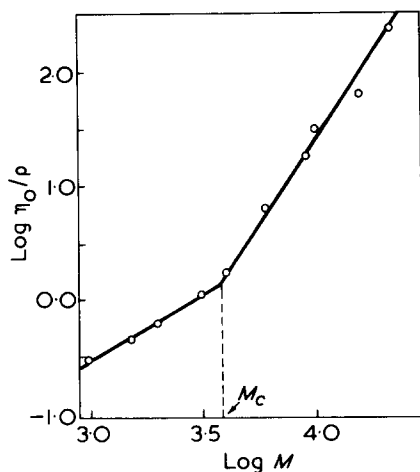


Figure 2 Logarithm of kinematic viscosity,  $\eta_0/\rho$ , at vanishing shear rate versus logarithm of molecular weight of PEO fractions at 70°C

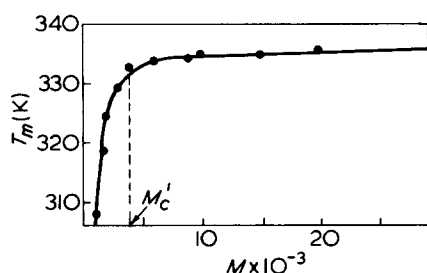


Figure 3 Melting point obtained by d.s.c. versus molecular weight of PEO fractions

molecular weight (sample PEO 2) and  $20 \times 10^3$  molecular weight (sample PEO 20) over the entire range of composition. All the samples, monodisperse fractions and blends, were also thermally characterized by differential scanning calorimetry (d.s.c.) using a Perkin-Elmer DSC-2B apparatus. The thermal characterization yielded the melting points, read at the position of the maxima of the fusion endotherm, and the apparent enthalpy of fusion obtained from the peak melting area (calibrated in cal/g against an indium standard).

#### Results and discussion

The cologarithm of kinematic viscosity  $\eta_0/\rho$  as function of  $1/T$  is reported in Figure 1 for the indicated monodisperse PEO fractions. In all cases a linear trend was observed and for each fraction it was possible to calculate the activation energy of viscous flow,  $\Delta E^*$ , from the slope of the respective straight line. This value appears to be almost constant with varying molecular weight and equal to 6.4 kcal/mol. This value has been used elsewhere<sup>1</sup> in a study of crystallization kinetics from the melt of the same

PEO fractions and their blends in place of the activation energy relative to the solid-liquid interfacial transport,  $\Delta F^*$ .

The latter term is usually calculated<sup>4</sup> by the WLF equation<sup>4</sup> based on the time-temperature superposition principle for viscoelastic materials. This equation, however, holds over a limited range of temperature going from the glass transition temperature ( $T_g$ ) up to  $T_g + 100^\circ\text{C}$ , whereas the isothermal crystallization of PEO has been obtained at low undercooling values and hence at crystallization temperatures  $T_c > T_g + 100^\circ\text{C}$ . It seems more convenient, therefore, to substitute  $\Delta F^*$  by the value of  $\Delta E^*$ , even though the latter has been experimentally obtained at temperatures greater than the melting point. The values of  $\Delta F_{\text{WLF}}$  range 7300 to 7700 cal/mol for  $T_c$  varying from 333 to 313K, respectively.

A log-log plot of the zero shear kinematic viscosity  $\eta_0/\rho$  as a function of logarithm of molecular weight  $M$ , calculated by intersecting the curves of Figure 1 with a vertical isotherm (at 70°C) is presented in Figure 2.

At any other temperature the resulting curve would be only slightly different since  $\Delta E^*$  does not vary with molecular weight.

In this Figure two limiting straight lines with very different slopes are clearly distinguishable. Their intersection defines a critical molecular weight,  $M_c$ , beyond which molecular entanglements begin to be effective.  $M_c$  is about equal to about 3600 for PEO and is almost independent of temperature. That this value is lower than values for other polymers<sup>5</sup> is reasonable since in comparison to them PEO has a higher flexibility.

The melting point  $T_m$  as a function of molecular weight for the PEO fractions is shown in Figure 3. It increases very sharply up to a critical molecular weight,  $M_c$ , of about 4000 and then remains constant. This behaviour can be interpreted assuming that the lower molecular weight fractions ( $M < 4000$ ) crystallize in the form of extended chains and the higher molecular weight fractions ( $M > 4000$ ) as folded chains<sup>6</sup>. In the former case the lamellar thickness is given by the length of the chain itself whereas in the latter case it is independent of molecular length and will depend only on the crystallization conditions (i.e. the degree of undercooling).

The apparent enthalpy of fusion calculated from the d.s.c. thermogram is

about 40 cal/g and does not change with varying molecular weight indicating that the degree of crystallinity is nearly constant for fractions lying in the range of molecular weights examined. For blends of PEO 2 and PEO 20 the viscous flow activation energy  $\Delta E^*$ , obtained from viscosity and density measurements, is the same as that of pure PEO fractions over the entire range of composition.

$\text{Log}(\eta_0/\rho)$  as function of  $\text{log } \nu$ , is shown in Figure 4 where  $\nu$  is the volume fraction of PEO 20 in the PEO 2-PEO 20 blend at a temperature of 70°C (or at any other temperature lying between 60° and 110°C). In this case it is possible by drawing two limiting straight lines corresponding to the viscous behaviour at low and high concentrations respectively, to define a critical volume fraction ( $\nu'_c \approx 0.30$ ), beyond which entanglement couplings become effective. D.s.c. thermograms of fusion for the same blends show a unique peak and the melting point is nearly constant up to a volume fraction,  $\nu'_c$ , of about 0.30 and then increases monotonically with increasing PEO 20 content (Figure 5), whereas the enthalpy of fusion remains constant over the entire range of composition and equal to that of all the above examined PEO fractions.

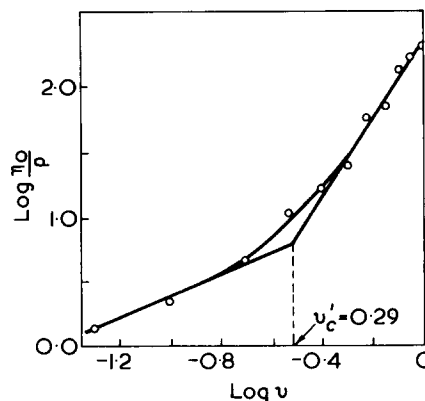


Figure 4 Logarithm of kinematic viscosity,  $\eta_0/\rho$ , versus logarithm of volume fraction of PEO 20 in the PEO 2-PEO 20 blend

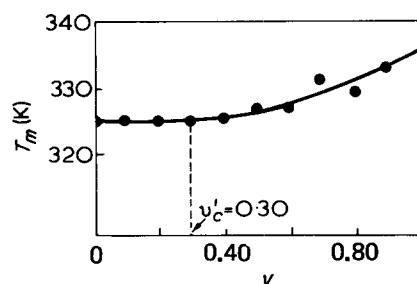


Figure 5 Melting point  $T_m$  obtained by d.s.c. versus volume fraction,  $\nu$ , of PEO 20 in the PEO 2-PEO 20 blend

## Conclusions

(1) There is a surprising analogy between the viscous behaviour at a vanishing shear rate in the melt and the thermal properties of fusion of PEO fractions and blends. In fact the critical parameters  $M_c$  and  $\nu_c$  relative to the entanglement coupling concept are very close in value to those at which presumably the PEO chains pass from chain extended to chain folded crystals ( $M'_c$  and  $\nu'_c$ ). This could be due to the nature of the chain, i.e. to its internal flexibility which beyond a certain length can give rise to folded chains (entanglements in one case and folded chain lamellae in the other). Of course

this fact could be due to coincidence and have no physical meaning.

(2) The viscosity data seem to show compatibility of the fraction in the blends over the entire range of composition in the melted state, since  $\Delta E^*$  results are independent of molecular weight and concentration.

(3) The d.s.c. data show compatibility of the PEO fractions in the solid state since there is a unique melting peak on the entire range of composition of the blend.

M. Costagliola, R. Greco and  
E. Martuscelli

(Laboratorio di Ricerche su Tecnologia  
dei Polimeri e Reologia,  
Arco Felice, Napoli, Italy)  
(Received 13 December 1977;  
revised 26 January 1978)

## References

- 1 Martuscelli, E. and Scafora, E. *Chim. Ind.* 1976, 58, 601
- 2 Cimino, S., Greco, R., Martuscelli, E. and Silvestre, G. *Polymer* submitted for publication
- 3 Hoffmann, J. D. *SPE Trans.* 1964, 4, 315
- 4 Williams, M. L., Landel, R. F. and Ferry, J. D. *J. Am. Chem. Soc.* 1955, 77, 3701
- 5 Ferry, J. D. 'Viscoelastic Properties of Polymers', 2nd Edn, Wiley, New York, 1970, p 409
- 6 Godowski, Y. K., Slonimski, G. L. and Garber, N. M. *J. Polym. Sci. (C)* 1972, 38, 1

## X-ray diffraction of processed poly(vinyl chloride)

X-ray diffraction traces have been obtained for both commercial PVC<sup>1-3</sup> and for materials having a higher level of syndiotacticity and crystallinity<sup>4-7</sup>.

Mammi and Nardi<sup>4</sup> have discussed the X-ray diffraction patterns obtained for oriented PVC fibres, and more recently Brady and Jabarin<sup>3</sup> have reported the changes in the wide-angle X-ray diffraction pattern of poly(vinyl chloride) introduced by uniaxially stretching at 23°C to the 'natural' draw ratio. This work prompts us to report some X-ray diffraction studies on PVC samples prepared by injection moulding, compression moulding and drawing above and below  $T_g$ .

Compression moulded sheets were prepared from a blend of 100 parts 'Corvic' D55/09 suspension polymer with 3 parts of a liquid organotin stabilizer ('Stanclere' T126). The blend was prepared using a Fielder mixer and moulded at 200°C for 10 min. The sheet was cooled in the mould to 40°C, cooling time being 20 min. Dumbell test pieces cut from the sheets were uniaxially oriented at a range of temperatures using an Instron tensile tester. The stretching rate used was 0.1 mm/min and the draw ratio was maintained constant at approximately 1.5 for all temperatures.

Injection moulded plaques were prepared using a Bipel injection moulding machine with the mould temperature at 40°C. The compound contained 'Breon' MSO/50 mass PVC polymer, 'Stanclere' T126 stabilizer, lubricants

(wax OP and calcium stearate) and processing aid (Paraloid K 120N).

Microscopical examination shows that sections cut through PVC injection moulded plaques have highly oriented 'skins', and a 'core' region in which the orientation is considerably less<sup>8</sup>. Samples of skin and core were prepared.

The X-ray diffraction measurements on all samples were made with Jeol DX-GE-2S generator and a DX-GO-S vertical goniometer using Ni-filtered  $\text{CuK}\alpha$  radiation in an air atmosphere. Reflectance mode measurements were made using rectangular samples (27 x 12 mm) not less than 0.60 mm thick.

For the stretched samples, measurements were made with the orientation direction at 0°, 45° and 90° to the plane containing the X-ray beam. Plots of intensity in arbitrary units versus diffraction angle,  $2\theta$ , were obtained over the range 12°–46°  $2\theta$ .

Figure 1 compares X-ray diffraction patterns for processed samples with that obtained for a compression moulded sample drawn at room temperature. The trace obtained for the compression moulding is similar to those previously reported<sup>1-3</sup> for PVC. For the injection moulded skin sample a significant increase in the peak at 17°  $2\theta$  compared with the compression moulded sample

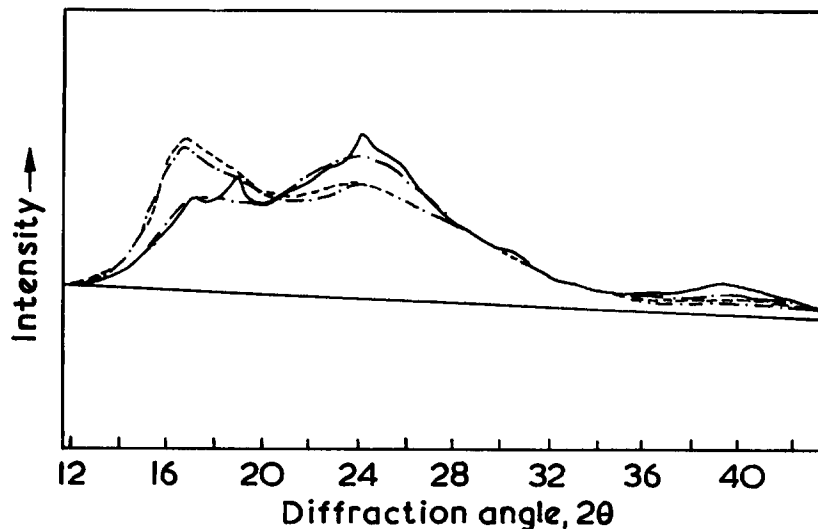


Figure 1 X-ray diffraction patterns for samples prepared by different processing techniques: —, compression moulded at 200°C; ---, injection moulded skin; - · - ·, uniaxially stretched at 23°C; · · · ·, injection moulded core